

Quantum Many-Body Mpemba Effect through Resonances

Shion Yamashika¹ and Ryusuke Hamazaki^{2,3}

¹*Department of Engineering Science, The University of Electro-Communications, Tokyo 182-8585, Japan.*

²*Nonequilibrium Quantum Statistical Mechanics RIKEN Hakubi Research Team, RIKEN Pioneering Research Institute (PRI), 2-1 Hirosawa, Wako, Saitama 351-0198, Japan*

³*RIKEN Center for Interdisciplinary Theoretical and Mathematical Sciences (iTHEMS), 2-1 Hirosawa, Wako, Saitama 351-0198, Japan*

Relaxation towards equilibrium is often assumed to be slower when a system starts farther from equilibrium, but this intuition fails in the Mpemba effect. Recent advances in controllable quantum platforms have enabled the exploration of its quantum analogue, the quantum Mpemba effect (QME), yet its microscopic origin remains largely unclear. Here we provide a general framework for understanding the QME in closed quantum many-body chaotic systems by reformulating the equilibration process of local subsystems in terms of Ruelle-Pollicott (RP) resonances. We show that suppressing the initial-state overlap with the dominant RP resonant mode accelerates subsystem equilibration and thereby yields the QME. We further uncover that a novel type of strong QME can occur via complete translation-symmetry breaking of initial states. We substantiate our predictions using the prototypical kicked Ising chain and exotic yet experimentally relevant initial states inspired by number theory. These findings cast the QME in closed many-body systems into a unified framework with open-system analogues and provide experimentally accessible signatures on state-of-the-art quantum platforms.

The Mpemba effect is an anomalous relaxation phenomenon, often summarised by the counterintuitive observation that hot water can freeze faster than cold water. Although reports of such phenomena date back to antiquity [1] and the effect was popularised in the modern literature after the rediscovery in the 1960s [2], it remains a longstanding puzzle in nonequilibrium physics. Proposed explanations range from evaporative cooling [3] to convection [4, 5], dissolved gases [6, 7], and supercooling [8]. However, the universal origin of the Mpemba effect remains under debate due to its very sensitivity to experimental setup [9, 10].

The remarkable development of quantum platforms has renewed interest in the Mpemba effect in quantum regimes [11–13]. In quantum systems, the endpoint of relaxation can be specified as a well-defined target state (for instance, a thermal state), and proximity to it can be rigorously quantified using standard measures of distance between density matrices [14–16]. This has led to the concept of the quantum Mpemba effect (QME), where, for the same dynamics, an initial state that is farther from the target state can nevertheless approach it faster than another initial state prepared closer. The QME not only provides a microscopic perspective on the anomalous relaxation, but also has practical relevance, for instance as a route to accelerated state preparation and cooling protocols in quantum platforms [17–19].

The QME has been widely studied both in open [20–25] and closed [26–31] quantum systems. However, its microscopic origin remains elusive beyond a few special cases, such as integrable systems [32] and Markovian open quantum systems [20]. This gap is particularly acute for generic closed quantum systems exhibiting many-body chaos [33, 34], where the whole system evolves unitarily and never relaxes while a local subsystem relaxes to a thermal equilibrium. Formulating a gen-

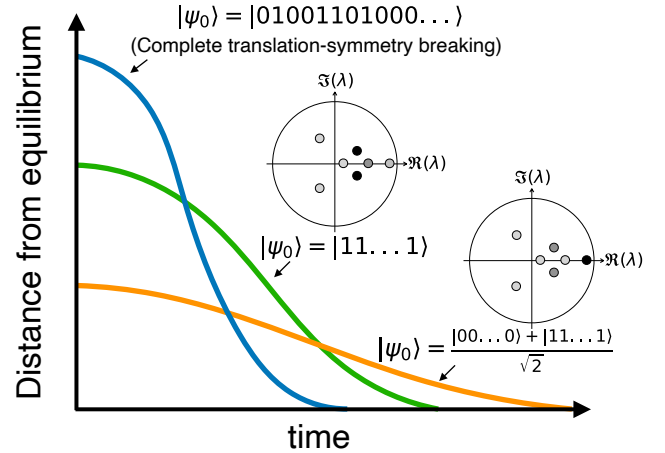


FIG. 1. **Quantum Mpemba effect through Ruelle-Pollicott resonances.** Late-time behaviour of a local subsystem in a closed quantum many-body chaotic system is controlled by the RP resonances, shown schematically as eigenvalues λ in the complex plane (insets). The resonant mode closest to the unit circle decays most slowly and sets the bottleneck for subsystem equilibration. Therefore, suppressing its initial-state overlap, encoded in the colour intensity of the spectral points in the insets, accelerates local equilibration and yields the QME. In addition, when the translational symmetry is completely broken by the initial state, equilibration can be further accelerated, giving rise to a strong QME.

eral description of such local equilibration is nontrivial, in contrast to the Markovian open quantum systems, where the equilibration process and the QME can be straightforwardly described by the Liouvillian spectrum [35, 36].

Here, we fill this gap and propose a universal mechanism of the QME in closed quantum many-body chaotic systems, which can be understood in close analogy with

the counterpart in Markovian open quantum systems. Our idea is to characterize local equilibration of the reduced density matrix in terms of Ruelle-Pollicott (RP) resonances, originally developed for describing correlation functions in classical chaos [37, 38] and recently extended to quantum many-body systems [39–41]. We uncover that the QME occurs when the initial state farther from equilibrium has a smaller overlap for slowly decaying RP resonant modes. Furthermore, the above general framework leads to the unconventional form of QME: strong QME via complete translation-symmetry breaking. That is, when the initial state completely breaks translational symmetry, the late-time relaxation law is qualitatively modified, so which state relaxes faster is solely governed by this modified relaxation law. Such complete translation-symmetry breaking emerges for novel yet experimentally relevant initial states constructed from “Legendre sequence”, well-known concept in number theory. Figure 1 provides a visualisation of these results. We support our predictions with numerical simulations of the kicked Ising chain, which can be realised in state-of-the-art experimental platforms [42–44].

Setup

We consider a chain of L qubits, whose state is described by the density matrix $\rho(t) = U^t \rho(0) U^{-t}$, where $\rho(0)$ is an initial state and U is the unitary time-evolution operator. As schematically shown in Fig. 2a, we decompose the whole system into local subsystem S of finite length ℓ and its complement E . The subsystem is described by the reduced density matrix

$$\rho_s(t) = \text{Tr}_E[\rho(t)] =: \mathcal{U}_t \rho_s(0). \quad (1)$$

Although the whole system never relaxes due to the unitarity of its dynamics, under typical circumstances, the subsystem relaxes into an equilibrium state at large times in the thermodynamic limit as $\lim_{t \rightarrow \infty} \lim_{L \rightarrow \infty} \rho_s(t) = \rho_s^{\text{eq}}$. In this context, the QME is said to occur when the subsystem that is initially farther from equilibrium relaxes faster than the one prepared closer to equilibrium.

If the reduced dynamics in equation (1) can be approximated as a Markovian dynamics generated by the time-independent Lindblad equation, the mechanism of the QME is understood from the spectral decomposition of the corresponding Liouvillian. That is, the initial state farther from equilibrium can relax faster simply because its overlap with the slowest decay mode is sufficiently small [13, 20, 21] (see Methods). Separately, in integrable quantum many-body systems, the QME can be understood in terms of the charge transport properties of quasiparticles [32]. However, in generic quantum many-body chaotic systems, such explanations fail because the reduced dynamics in equation (1) is typically non-Markovian and lacks the quasiparticle description. We here resolve this problem and show that the QME in closed quantum many-body chaotic systems can be

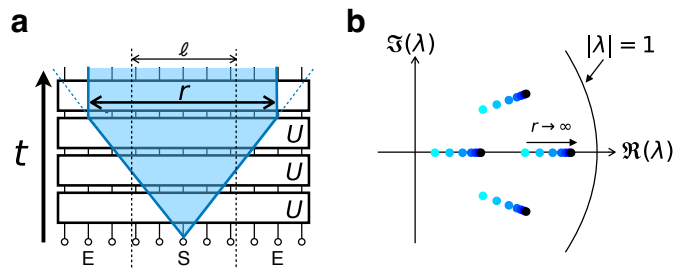


FIG. 2. **Truncated propagator and RP resonances.** **a**, Under the truncated propagator $\bigoplus_k \mathcal{E}_{k,r}$, any local observable increases its spatial extent strictly within the light cone until its support length reaches the cutoff r . **b**, As r increases, the eigenvalues of $\mathcal{E}_{k,r}$ approach the unit circle because its original counterpart is unitary. The RP resonances are the eigenvalues that remain strictly inside the unit circle even in the limit $r \rightarrow \infty$.

understood within the framework analogous to that for Markovian dynamics, through the RP resonances.

In what follows, we consider the global unitary dynamics U that is translationally invariant. We assume that the adjoint propagator $\mathcal{E}(\cdot) = U^\dagger(\cdot)U$ transforms a local operator to another local operator strictly within the light cone (see Fig. 2a). We resolve it into quasi-momentum sectors k , $\mathcal{E} = \bigoplus_k \mathcal{E}_k$, where \mathcal{E}_k is restriction of \mathcal{E} to the operator subspace spanned by Fourier-transformed operators $O_k := \sum_{j \in \mathbb{Z}} e^{-ikj} \mathcal{T}^j O$, with \mathcal{T} being the one-site translation map. For simplicity we assume one-site translation invariance of U , but the same construction extends straightforwardly to dynamics with a finite spatial periodicity (e.g., brickwork circuits invariant under two-site translations) by working with the corresponding reduced Brillouin zone and momentum sectors (see, e.g., Ref. [40]).

RP resonances can be obtained by introducing a cutoff r on operator size by defining a truncated propagator $\mathcal{E}_{k,r} = \Pi_{k,r} \mathcal{E}_k \Pi_{k,r}$ (see Fig. 2a) [39, 40], where $\Pi_{k,r}$ denotes the projection onto the operator subspace spanned by $\{P_k | P \in \mathcal{P}_r\}$. Here \mathcal{P}_r is the set of Pauli strings supported on at most r consecutive qubits starting from the leftmost site of subsystem S . Although \mathcal{E}_k is strictly unitary, some eigenvalues of $\mathcal{E}_{k,r}$ do not approach unity even when r increases, as illustrated schematically in Fig. 2b. The RP resonances are defined as those eigenvalues that remain strictly inside the unit circle even in the limit $r \rightarrow \infty$.

QME through RP resonances

Our central result is an asymptotic expansion of the reduced density matrix in terms of RP resonances. In the thermodynamic limit $L \rightarrow \infty$, we find for large t that

$$\rho_s(t) \simeq \frac{I}{2^\ell} + \sum_{\alpha} \int_{-\pi}^{\pi} \frac{dk}{2\pi} \lambda_{\alpha,k}^t \text{Tr}[\rho(0) V_{\alpha,k}^{\text{R}}] \varrho_{\alpha,k}. \quad (2)$$

Here $\lambda_{\alpha,k}$ and $V_{\alpha,k}^{\text{L(R)}}$ are an eigenvalue and the corresponding left (right) eigenoperator of $\mathcal{E}_{k,r}$, with $\lambda_{\alpha,k}$ or-

dered in decreasing absolute value. The symbol \simeq in equation (2) reflects the finite cutoff r ; the relation becomes exact in the limit $r \rightarrow \infty$. The operator $\varrho_{\alpha,k}$ acts only on the subsystem S , see Methods for its explicit expression. Importantly, $\varrho_{\alpha,k}$ depends solely on $V_{\alpha,k}^L$ and on the subsystem geometry, whereas all dependence on the initial condition enters through the overlap function $\text{Tr}[\rho(0)V_{\alpha,k}^R]$. The proof of equation (2) is presented in Methods.

When the initial state is invariant under l -site translations, i.e., $\mathcal{T}^l \rho(0) = \rho(0)$, the overlap function in equation (2) develops delta-function peaks at the discrete momenta $\Lambda_l = \{2\pi n/l \mid n = 0, 1, \dots, l-1\}$ as $\text{Tr}[\rho(0)V_{\alpha,k}^R] = 2\pi c_{\alpha,k} \sum_{q \in \Lambda_l} \delta(k-q)$, where $c_{\alpha,k}$ are the weights of the resonant modes (fixed solely by $\rho(0)$; see Methods for the explicit expression). As a consequence, the k -integral in equation (2) reduces to a finite sum and the reduced density matrix takes the form

$$\rho_s(t) \simeq \rho_s^{\text{eq}} + \sum_{k \in \Lambda_l} \sum_{\alpha: |\lambda_{\alpha,k}| < 1} \lambda_{\alpha,k}^t c_{\alpha,k} \varrho_{\alpha,k}. \quad (3)$$

Here, the stationary part ρ_s^{eq} is determined by the modes with $\lambda_{\alpha,k} = 1$,

$$\rho_s^{\text{eq}} = \frac{I}{2^\ell} + \sum_{k \in \Lambda_l} \sum_{\alpha: \lambda_{\alpha,k} = 1} c_{\alpha,k} \varrho_{\alpha,k}. \quad (4)$$

Equation (3) shows that the large-time behaviour of $\rho_s(t)$ is governed by a finite set of effective decay modes associated with the RP resonances. This allows us to understand the QME in the closed quantum many-body chaotic system in direct analogy with the Markovian case. At large times, the subsystem dynamics is governed by the slowest decay mode, namely the RP resonance with the largest absolute value $|\lambda_{\alpha,k}|$. Consequently, a system that is initially farther from equilibrium can nevertheless relax faster if the weight of this slowest mode in the initial state, $|c_{\alpha,k}|$, is smaller.

A crucial difference from the Markovian case is that, in general, the weights $c_{\alpha,k}$ of the decay modes, and therefore the condition for the QME to occur, are determined not by the initial state of the subsystem of interest, $\rho_s(0)$, but by that of the global system, $\rho(0)$. In addition, when the global dynamics U has a conserved quantity Q , one has $\mathcal{E}Q = Q$, which implies the presence of an eigenvalue $\lambda_{\alpha,k} = 1$ [45] and therefore makes the equilibrium state (4) dependent on the initial state, even if the reduced dynamics in equation (1) has no conserved quantities. These features reflect the non-Markovian nature of the reduced dynamics in equation (1).

QME in kicked Ising chain

While the framework presented above generally holds whenever the unitary dynamics is translationally invariant and has the local structure, we now apply it to a concrete example. Specifically, we focus on the chaotic kicked Ising chain, whose one-step dynamics is given by

$$U = e^{i\tau \sum_i h_x X_i} e^{i\tau \sum_i (J Z_i Z_{i+1} + h_z Z_i)}, \quad (5)$$

where $\{X_i, Y_i, Z_i\}$ are the Pauli matrices acting on the i -th qubit. For generic values of parameters (τ, h_x, h_z) , the kicked Ising chain has no conserved quantity, which implies $|\lambda_{1,k}| < 1$ for all k , and hence the subsystem relaxes into the infinite-temperature state $\rho_s^{\text{eq}} = I/2^\ell$ [46, 47].

The RP resonances of the kicked Ising chain (5) have been studied in Ref. [40], where it was shown that $|\lambda_{1,k}|$ attains its global maximum at $k = 0$ and $\lambda_{1,0} \in \mathbb{R}$. It then follows from equation (3) that the reduced density matrix for the subsystem behaves at large times as

$$\rho_s(t) \simeq \frac{I}{2^\ell} + \lambda_{1,0}^t c_{1,0} \varrho_{1,0}. \quad (6)$$

This expression shows that the QME occurs when the global initial state of the system that is initially closer to equilibrium has a larger weight $|c_{1,0}|$ of the dominant RP resonance at $k = 0$.

To make the above prediction more concrete, we consider a family of initial states of the form $\rho(0) = |\theta\rangle\langle\theta|$, where

$$|\theta\rangle = \cos\left(\frac{\theta}{2}\right) |00\dots 0\rangle + \sin\left(\frac{\theta}{2}\right) |11\dots 1\rangle, \quad (7)$$

with $\theta \in [0, \pi]$. We quantify the distance to equilibrium using the Bures distance [15],

$$D(t) := \sqrt{2\left(1 - \text{Tr}\sqrt{\sqrt{\rho_s^{\text{eq}}}\rho_s(t)\sqrt{\rho_s^{\text{eq}}}}\right)}. \quad (8)$$

It quantifies how distinguishable two density matrices are (see Methods).

On one hand, as shown in Fig. 3a, $D(0)$ for the initial state (7) attains its minimum at $\theta = \pi/2$ and the subsystem is initially closer to equilibrium when θ lies closer to $\pi/2$. On the other hand, Fig. 3b shows the θ -dependence of $|c_{1,0}|$, which is computed by numerically diagonalising $\mathcal{E}_{k,r}$ (see Methods), for the same family of initial states. We find that $|c_{1,0}|$ is maximal at $\theta = 0$ and decreases as θ increases, indicating faster equilibration as θ approaches π . Taken together, these trends imply that the QME occurs for a pair of initial states with angles θ_i ($i = \text{I}, \text{II}$) if and only if the following two conditions are satisfied: (i) $|\theta_{\text{I}} - \pi/2| < |\theta_{\text{II}} - \pi/2|$ and (ii) $\theta_{\text{I}} < \theta_{\text{II}}$.

We test these results in Fig. 3c, in which we plot by solid curves the time evolution of $D(t)$ for the initial states (7) with several values of θ , for the kicked Ising chain of length $L = 24$ with periodic boundary conditions. It shows that curves corresponding to different values of θ intersect at certain times, signaling the occurrence of the QME. As expected, such intersections are observed only for pairs of initial states that satisfy both conditions (i) and (ii). The inset further shows that the exact numerical results (solid curves) approach the asymptotic form of $D(t)$ calculated from equation (6) (dotted curves) at late times. The residual discrepancy between the solid and dotted curves for small θ originates

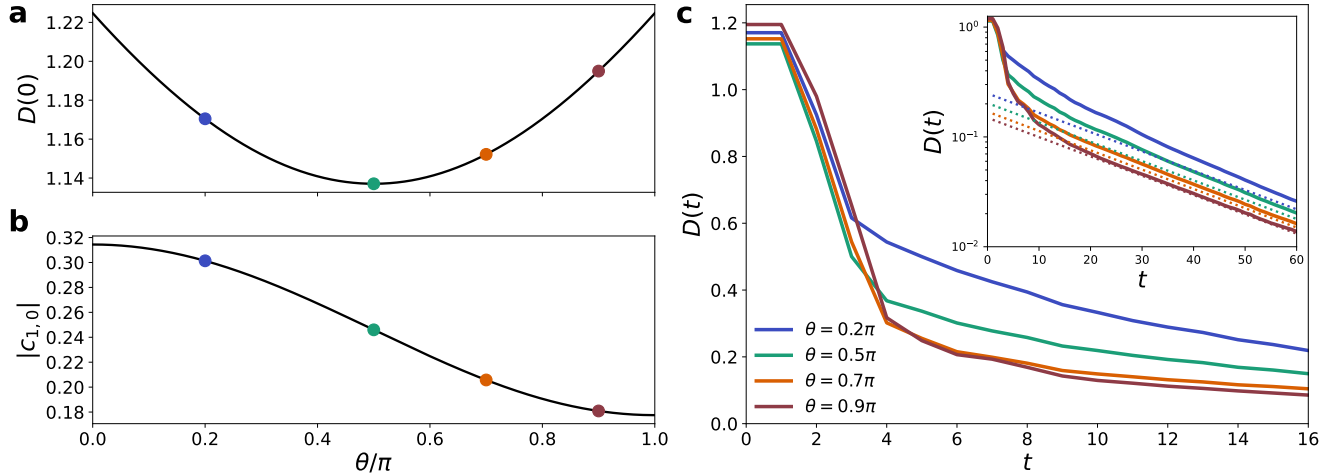


FIG. 3. **The QME in the dynamics of the kicked Ising chain.** **a**, The Bures distance $D(0)$ for the initial state (7). It quantifies how far the system is from equilibrium at $t = 0$. **b**, Weight $|c_{1,0}|$ of slowest decay mode (the dominant RP resonance) for the same initial state. As $|c_{1,0}|$ decreases, the subsystem equilibrates faster. **c**, Time evolution of the Bures distance under the dynamics of the kicked Ising chain. The solid curves correspond to the time evolution from the initial state in equation (7). Inset shows the results for large times, in which the asymptotic forms of $D(t)$ predicted by equation (6) are plotted as the dotted curves. We set $(\tau, h_x, h_z) = (0.65, 0.9, 0.8)$, subsystem size $\ell = 4$, and system size $L = 24$ with periodic boundary conditions for all the plots. To obtain the solid curve in **b** and the dotted curves in the inset of **c**, we evaluate $\lambda_{1,k}$, $c_{1,k}$, and $\text{Tr}[\rho(0)V_{1,k}^R]$ by numerically diagonalising $\mathcal{E}_{k,r}$ with $r = 12$ (see Methods). The values of θ used in **c** are indicated by the filled circles in **a** and **b**.

from the truncation at finite r used to extract $c_{1,0}$ and $\lambda_{1,0}$ from $\mathcal{E}_{k,r}$.

Strong QME via translational symmetry

While equation (3) suggests that the subsystem relaxes exponentially toward equilibrium, similarly to the Markovian case, this description breaks down when the initial state $\rho(0)$ completely breaks translational symmetry, i.e., when $\mathcal{T}^l \rho(0) \neq \rho(0)$ for any integer l . In the translationally invariant case, the overlap factor $\text{Tr}[\rho(0)V_{\alpha,k}^R]$ exhibits delta-function peaks, so that the k -integral in equation (2) reduces to a discrete sum. By contrast, when translational symmetry is absent, no such delta-function peaks are present in $\text{Tr}[\rho(0)V_{\alpha,k}^R]$ and hence the contributions from the RP resonances are distributed over a continuum of momenta (see Fig. 4a). In this case, the large-time behaviour of the reduced density matrix is obtained by evaluating the integral over k in equation (2) via the method of steepest descent [48], yielding

$$\rho_s(t) \simeq \frac{I}{2^\ell} + \sum_{\alpha} \sum_{k \in \Sigma_{\alpha}} \frac{\lambda_{\alpha,k}^t \text{Tr}[\rho(0)V_{\alpha,k}^R] \varrho_{\alpha,k}}{\sqrt{2\pi t \nu''_{\alpha,k}}} e^{-\frac{t|\nu'_{\alpha,k}|^2}{2\nu''_{\alpha,k}}}, \quad (9)$$

where $\nu_{\alpha,k} = -\ln \lambda_{\alpha,k}$, $' = \partial_k$, and Σ_{α} is the set of points at which $|\lambda_{\alpha,k}|$ attains its local maxima. The derivation of equation (9) is provided in the Supplemental Information.

Equation (9) highlights that complete translation-symmetry breaking qualitatively reshapes the relaxation

law in two ways. First, the dominant resonant mode is no longer selected from the discrete momenta Λ_l imposed by spatial periodicity of the initial state; instead it is determined by the set Σ_{α} of the points at which $|\lambda_{\alpha,k}|$ takes its local maxima. Second, $\rho_s(t)$ acquires an algebraic prefactor $t^{-1/2}$ compared with the purely exponential form in equation (3). Moreover, when $\nu'_{\alpha,k} \neq 0$ for $k \in \Sigma_{\alpha}$, an additional exponential decay factor appears. In the Supplemental Information we further show that the relaxation can be faster when the initial state satisfies $\text{Tr}[\rho(0)V_{\alpha,k}^R] = 0$ for $k \in \Sigma_{\alpha}$. In that case the algebraic prefactor is replaced by $t^{-\frac{1+\gamma}{2}}$ with $\gamma \geq 1$. These features imply that complete translational-symmetry breaking can induce a strong QME, where which state equilibrates faster is governed by the modified relaxation law, rather than by a mere difference in their overlaps with the same slowest mode.

We now return to the kicked Ising chain in equation (5) to make the above argument explicit. As noted before, $|\lambda_{1,k}|$ for this model attains its global maximum at $k = 0$ and $\lambda_{1,k} \in \mathbb{R}$ in the vicinity of $k = 0$. Equation (9) therefore reduces to

$$\rho_s(t) \simeq \frac{I}{2^\ell} + \frac{\lambda_{1,0}^t \text{Tr}[\rho(0)V_{1,0}^R] \varrho_{1,0}}{\sqrt{2\pi t \nu''_{1,0}}}. \quad (10)$$

Comparing this expression with equation (6), one readily finds that the relaxation in the kicked Ising dynamics is accelerated when the initial state completely breaks translational symmetry.

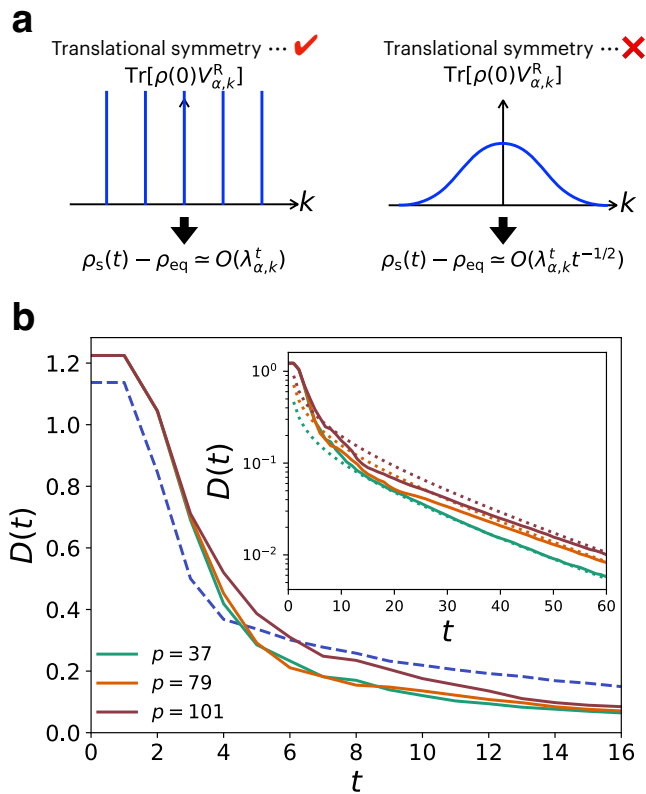


FIG. 4. Strong QME from complete breaking of translational symmetry. **a**, Schematic contrast in the profile of the overlap function $\text{Tr}[\rho(0)V_{\alpha,k}^R]$. For an initial state with translational symmetry, the overlap develops discrete delta-function peaks at selected momenta, resulting in the purely exponential equilibration. By contrast, when translational symmetry is completely broken in the initial state, the overlap is instead spread over a continuum of momenta, which results in the accelerated equilibration with factor $t^{-1/2}$ in the case of the kicked Ising chain. **b**, Time evolution of $D(t)$ for the kicked Ising model starting from the initial states constructed from Legendre sequences (solid curves, different primes p), which decay faster than that for a translationally invariant initial state (7) (dashed curve, $\theta = \pi/2$). Inset represents the results for late times, in which the asymptotic forms of $D(t)$ predicted by equation (10) are plotted as the dotted curves. To obtain the dotted curves in **b**, we evaluate $\lambda_{1,k}$ and $\text{Tr}[\rho(0)V_{1,k}^R]$ by numerically diagonalising $\mathcal{E}_{k,r}$ with $r = 12$. We set $(\tau, h_x, h_z) = (0.65, 0.9, 0.8)$, subsystem size $\ell = 4$, and system size $L = 24$ with periodic boundary conditions for all the plots.

For the numerical test of the above results, we introduce an exotic class of deterministic initial product states generated from the Legendre sequence [49], a famous concept in number theory. Fix a prime number p , and define a bit string $\{s_n\}$ by $s_n = 0$ if n is a quadratic residue modulo p (i.e., there exists an integer m such that $m^2 \equiv n \pmod{p}$) and $s_n = 1$ otherwise; for instance, 01001101... for $p = 37$ and 00100110... for $p = 79$. We then take the first L bits $\{s_n\}_{n=0}^{L-1}$ and use them as a computational basis configuration corresponding to the

initial state, i.e., $\rho(0) = \bigotimes_{n=0}^{L-1} |s_n\rangle\langle s_n|$. Such states can easily be prepared experimentally by single-qubit initialisation in the Z basis. Varying p generates many distinct initial states that completely break translational symmetry without introducing any randomness, providing a reproducible route to probe the strong QME. Although the sequence is periodic with period p by construction, we choose $p > L$ so that no repetition occurs in the system we numerically simulate.

We can see in Fig. 4b that such number-theoretic patterns in the initial condition indeed reshape the relaxation law of local equilibration, where we plot by solid curves the time evolution of $D(t)$ for the initial states generated from the Legendre sequence with several choices of prime p . These numerical results agree well with the asymptotic form predicted by equation (10) at late times, and show that they decay faster than that for the translationally invariant initial state (7) (dashed curve). This provides a direct numerical demonstration of the strong QME rooted in the complete breaking of translational symmetry.

Discussion

To summarise, we have shown that the QME in closed quantum many-body chaotic systems can be understood within the framework of RP resonances. These resonances govern the relaxation of local subsystems, and the QME occurs when the state initially farther from equilibrium carries a smaller weight of the dominant (slowest) resonant mode. We have also shown that a complete breaking of translational symmetry in the initial state can qualitatively reshape the late-time relaxation law and induce a strong QME: which initial state equilibrates faster is then dictated by this change in the asymptotic relaxation behavior, rather than by a mere difference in their overlaps with the same slowest mode.

Our predictions agree with numerical simulations of the kicked Ising chain at experimentally accessible sizes, even though RP resonances are rigorously defined only in the thermodynamic limit [41]. The kicked Ising chain has already been realised in a variety of experimental platforms, such as trapped ions and superconducting quantum processors [42–44], and the initial states considered here, including the novel ones inspired by number theory, can be prepared with current technology. An experimental test would directly probe the mechanism of local equilibration in quantum many-body chaotic systems through RP resonances.

More broadly, the present formalism provides a route to analyse late-time local relaxation beyond the QME by giving access to the reduced density matrix rather than a particular observable. In particular, it enables principled predictions for the late-time behaviour of non-linear functionals of density matrices, such as quantum Fisher information, Rényi entanglement entropies, and other information-theoretic quantities, which are not captured by tracking any single observable. It will also be interesting to extend our framework to continuous-time

Hamiltonian dynamics, where one expects an analogous mode picture to govern late-time local equilibration, now shaped by energy conservation and the hydrodynamic slow modes. Another direction is to explore long-range interacting systems, where locality and the effective light cone are modified; understanding how the resonance picture adapts may reveal new late-time relaxation laws.

Methods

QME in Markovian open quantum systems. If the reduced dynamics in equation (1) can be approximated as Markovian, so that it forms a semigroup $\mathcal{U}_t \mathcal{U}_{t'} = \mathcal{U}_{t+t'}$ ($t, t' > 0$), the mechanism of the QME becomes transparent. In this case $\rho_s(t)$ obeys the Gorini-Kossakowski-Sudarshan-Lindblad (GKSL) master equation [35, 36],

$$\dot{\rho}_s(t) = -\mathcal{L}\rho_s(t), \quad (11)$$

where \mathcal{L} is a Liouvillian superoperator. Then, under natural assumptions such as uniqueness of the equilibrium state, $\rho_s(t)$ can be written at large times as

$$\rho_s(t) \simeq \rho_s^{\text{eq}} + e^{-\mu_{\text{sl}} t} \rho_{\text{sl}} \text{Tr}[\rho_s(0) \pi_{\text{sl}}^\dagger]. \quad (12)$$

Here, μ_{sl} is the eigenvalue of \mathcal{L} with smallest nonzero real part, which we here assume to be real for simplicity, and π_{sl} (ρ_{sl}) denotes the corresponding left (right) eigenvectors. As a consequence, a subsystem that is initially farther from equilibrium can nevertheless relax faster, for the simple reason that its overlap with the slowest decay mode, $\text{Tr}[\rho_s(0) \pi_{\text{sl}}^\dagger]$, is sufficiently small [13, 20, 21].

Asymptotic expression of density matrix. Here we provide the derivation of equations (2) and (3). Without loss of generality, $\rho_s(t)$ can be written as

$$\rho_s(t) = \frac{1}{2^\ell} \left(I + \sum_{i=0}^{\ell-1} \sum_{P \in \mathcal{P}_{\ell-i}} \text{Tr}[\rho(t) \mathcal{T}^i P] \mathcal{T}^i P \right). \quad (13)$$

Using the Fourier transform $P_k = \sum_{i \in \mathbb{Z}} e^{-iki} \mathcal{T}^i P$, the trace in the above equation can be rewritten as

$$\text{Tr}[\rho(t) \mathcal{T}^i P] = \int_{-\pi}^{\pi} \frac{dk}{2\pi} e^{iki} \text{Tr}[\rho(t) P_k]. \quad (14)$$

For large times, $\text{Tr}[\rho(t) P_k]$ can be expressed in terms of RP resonant modes as [39, 40]

$$\text{Tr}[\rho(t) P_k] \simeq \sum_{\alpha} \lambda_{\alpha,k}^t v_{\alpha,P_k}^L \text{Tr}[\rho(0) V_{\alpha,k}^R]. \quad (15)$$

Here, $\lambda_{\alpha,k}$ denote the eigenvalues of $\mathcal{E}_{k,r}$ and $V_{\alpha,k}^{\text{L(R)}} = \sum_{P \in \mathcal{P}_r} v_{\alpha,P_k}^{\text{L(R)}} P_k$ are the corresponding left (right) eigenvectors. We order $\lambda_{\alpha,k}$ by decreasing absolute value and adopt the bi-orthonormal convention such that $\sum_{P \in \mathcal{P}_r} (v_{\alpha,P_k}^L)^* v_{\beta,P_k}^R = \delta_{\alpha,\beta}$. Substituting equations (14) and (15) into equation (13), we arrive at equation (2) with

$$\rho_{\alpha,k} = \frac{1}{2^\ell} \sum_{i=0}^{\ell-1} \sum_{P \in \mathcal{P}_{\ell-i}} e^{iki} v_{\alpha,P_k}^L \mathcal{T}^i P. \quad (16)$$

Equation (3) further simplifies when $\mathcal{T}^l \rho(0) = \rho(0)$ for some integer l . For such initial states, the overlap function $\text{Tr}[\rho(0) V_{\alpha,k}^R]$ reduces to

$$\text{Tr}[\rho(0) V_{\alpha,k}^R] = 2\pi c_{\alpha,k} \sum_{q \in \Lambda_l} \delta(k - q), \quad (17)$$

where

$$c_{\alpha,k} = l^{-1} \sum_{i=0}^{l-1} \sum_{P \in \mathcal{P}_r} v_{\alpha,P_k}^R \text{Tr}[\rho(0) \mathcal{T}^i P] e^{-iki}. \quad (18)$$

Substituting equation (17) into equation (2) and performing the integral over k , we obtain equation (3).

Truncated propagator. Here, we describe an explicit construction of $\mathcal{E}_{k,r}$. The following arguments are based on Ref. [40]. We assume that U generates two-local dynamics, such that $\mathcal{E}(\cdot) = U^\dagger(\cdot)U$ enlarges the support of any operator by at most one qubit to the left and to the right (extension to general strictly local dynamics is straightforward, see, e.g., Ref. [40]). Then, for a Pauli string $P \in \mathcal{P}_r$, $\mathcal{E}P$ can be expanded as a linear combination of Pauli strings,

$$\begin{aligned} \mathcal{E}P &= \sum_{P' \in \mathcal{P}_r} (M_{P,P'} + M_{P,\mathcal{T}P'} \mathcal{T} + M_{P,\mathcal{T}^{-1}P'} \mathcal{T}^{-1}) P' \\ &+ \sum_{P' \in \mathcal{P}_{r+1} \setminus \mathcal{P}_r} (M_{P,P'} + M_{P,\mathcal{T}^{-1}P'} \mathcal{T}^{-1}) P' \\ &+ \sum_{P' \in \mathcal{P}_{r+2} \setminus \mathcal{P}_{r+1}} M_{P,\mathcal{T}^{-1}P'} \mathcal{T}^{-1} P', \end{aligned} \quad (19)$$

with $\{M_{P,P'}\}$ being the expansion coefficients. Performing the Fourier transform, it reduces to

$$\begin{aligned} \mathcal{E}_k P_k &= \sum_{P' \in \mathcal{P}_r} (M_{P,P'} + M_{P,\mathcal{T}P'} e^{ik} + M_{P,\mathcal{T}^{-1}P'} e^{-ik}) P'_k \\ &+ \sum_{P' \in \mathcal{P}_{r+1} \setminus \mathcal{P}_r} (M_{P,P'} + M_{P,\mathcal{T}^{-1}P'} e^{-ik}) P'_k \\ &+ \sum_{P' \in \mathcal{P}_{r+2} \setminus \mathcal{P}_{r+1}} M_{P,\mathcal{T}^{-1}P'} e^{-ik} P'_k. \end{aligned} \quad (20)$$

Its projection onto the operator subspace spanned by $\{P_k | P \in \mathcal{P}_r\}$ can be obtained by neglecting the second and the third term in the above equation, yielding

$$\begin{aligned} \mathcal{E}_{k,r} P_k &= \sum_{P' \in \mathcal{P}_r} (M_{P,P'} + M_{P,\mathcal{T}P'} e^{ik} \\ &+ M_{P,\mathcal{T}^{-1}P'} e^{-ik}) P'_k. \end{aligned} \quad (21)$$

Using equation (21), we extract the RP resonances and the corresponding eigenoperators by numerically diagonalising $\mathcal{E}_{k,r}$. This strategy is justified by the strict locality of U , which guarantees that the action of \mathcal{E}_k is recovered from $\mathcal{E}_{k,r}$ once r is taken sufficiently large. The numerical results in the main text are obtained by

diagonalising $\mathcal{E}_{k,r}$ with $r = 12$, which is the largest cutoff accessible in our numerics.

Bures distance. Throughout the paper, we employ the Bures distance (8) to quantify the distance from equilibrium of the subsystem. The Bures distance has good properties as a measure of how close the subsystem is to the equilibrium state: it is non-negative $D(t) \geq 0$ and vanishes if and only if $\rho_s(t) = \rho_s^{\text{eq}}$.

For the kicked Ising chain, we can explicitly derive the asymptotic form of the Bures distance at large times by using the fact that the equilibrium state is $\rho_s^{\text{eq}} = I/2^\ell$. In this case, the right-hand side of equation (8) can be expanded in terms of $\delta\rho_s(t) = \rho_s(t) - \rho_s^{\text{eq}}$ as

$$D(t) \simeq 2^{\ell/2-1} \sqrt{\text{Tr}[\delta\rho_s(t)^2]}. \quad (22)$$

Substituting equation (6) into the above equation, we obtain

$$D(t) \simeq 2^{\ell/2-1} |c_{1,0}| |\lambda_{1,0}|^t \sqrt{\text{Tr}[\varrho_{1,0}^2]}, \quad (23)$$

which applies when $\rho(0)$ has translational symmetry or spatial periodicity with finite period (note that $\varrho_{1,0}$ is Hermitian for our model). On the other hand, when $\rho(0)$ completely breaks the translational symmetry, the Bures distance at large times can be obtained by substituting

equation (10) into equation (22) as

$$D(t) \simeq \frac{2^{\ell/2-1} |\text{Tr}[\rho(0)V_{1,0}^R]| |\lambda_{1,0}|^t \sqrt{\text{Tr}[\varrho_{1,0}^2]}}{\sqrt{2\pi\nu'_{1,0}t}}. \quad (24)$$

The dotted curves in the inset of Figs. 3c and 4b are obtained by evaluating equations (23) and (24).

Data availability

The data that support the plots within this paper are provided in the Source Data file.

Code availability

The computer codes used to generate the results that are reported in this paper are available from the authors upon reasonable request. All correspondence and requests for materials can be addressed to any of the authors.

Acknowledgements

S.Y. was supported by Grant-in-Aid for Young Scientists (Start-up) No.25K23355 and Institute for Advanced Science, University of Electro-Communications. R.H. was supported by JSPS KAKENHI Grant No. JP24K16982 and by JST ERATO Grant Number JP-MJER2302, Japan.

Author Contributions

S.Y. and R.H. contributed to developing the theory, interpreting the results, and writing the manuscript. S.Y. performed the numerical simulations and analytic computations.

Competing interests

The authors declare no competing interests.

-
- [1] Aristotle, *Meteorologica* (Clarendon Press, Oxford, 1923).
- [2] E. B. Mpemba and D. G. Osborne, Cool?, *Physics Education* **4**, 172 (1969).
- [3] M. Vynnycky and S. L. Mitchell, Evaporative cooling and the mpemba effect, *Heat and Mass Transfer* **46**, 881 (2010).
- [4] M. Vynnycky and N. Maeno, Axisymmetric natural convection-driven evaporation of hot water and the mpemba effect, *International Journal of Heat and Mass Transfer* **55**, 7297 (2012).
- [5] M. Vynnycky and S. Kimura, Can natural convection alone explain the mpemba effect?, *International Journal of Heat and Mass Transfer* **80**, 243 (2015).
- [6] B. Wojciechowski, I. Owczarek, and G. Bednarz, Freezing of aqueous solutions containing gases, *Crystal Research and Technology* **23**, 843 (1988).
- [7] W. B. Zimmerman, In search of a mpemba effect protocol: Some hot water does cool and freeze faster than cold, *Chemical Engineering Science* **247**, 117043 (2022).
- [8] D. Auerbach, Supercooling and the mpemba effect: When hot water freezes quicker than cold, *American Journal of Physics* **63**, 882 (1995).
- [9] H. C. Burridge and P. F. Linden, Questioning the mpemba effect: hot water does not cool more quickly than cold, *Scientific Reports* **6**, 37665 (2016).
- [10] H. C. Burridge and O. Hallstadius, Observing the mpemba effect with minimal bias and the value of the mpemba effect to scientific outreach and engagement, *Proceedings of the Royal Society A: Mathematical, Physical and Engineering Sciences* **476**, 476 (2020).
- [11] L. K. Joshi, J. Franke, A. Rath, F. Ares, S. Murciano, F. Kranzl, R. Blatt, P. Zoller, B. Vermersch, P. Calabrese, C. F. Roos, and M. K. Joshi, Observing the quantum mpemba effect in quantum simulations, *Physical Review Letters* **133**, 010402 (2024).
- [12] S. Aharony Shapira, Y. Shapira, J. Markov, G. Teza, N. Akerman, O. Raz, and R. Ozeri, Inverse mpemba effect demonstrated on a single trapped ion qubit, *Physical Review Letters* **133**, 010403 (2024).

- [13] J. Zhang, G. Xia, C.-W. Wu, T. Chen, Q. Zhang, Y. Xie, W.-B. Su, W. Wu, C.-W. Qiu, P.-X. Chen, W. Li, H. Jing, and Y.-L. Zhou, Observation of quantum strong mpemba effect, *Nature Communications* **16**, 301 (2025).
- [14] R. Jozsa, Fidelity for mixed quantum states, *Journal of Modern Optics* **41**, 2315 (1994).
- [15] M. Hübner, Explicit computation of the bures distance for density matrices, *Physics Letters A* **163**, 239 (1992).
- [16] C. Fuchs and J. van de Graaf, Cryptographic distinguishability measures for quantum-mechanical states, *IEEE Transactions on Information Theory* **45**, 1216 (1999).
- [17] F. Ares, P. Calabrese, and S. Murciano, The quantum mpemba effects, *Nature Reviews Physics* **7**, 451 (2025).
- [18] P. Westhoff, S. Paeckel, and M. Moroder, Fast and direct preparation of a genuine lattice bose-einstein condensate via the quantum mpemba effect, *Physical Review A* **112**, L061304 (2025).
- [19] M. Boubakour, S. Endo, T. Fogarty, and T. Busch, Dynamical invariant based shortcut to equilibration in open quantum systems, *Quantum Science and Technology* **10**, 025036 (2025).
- [20] F. Carollo, A. Lasanta, and I. Lesanovsky, Exponentially accelerated approach to stationarity in markovian open quantum systems through the mpemba effect, *Physical Review Letters* **127**, 060401 (2021).
- [21] M. Moroder, O. Culhane, K. Zawadzki, and J. Goold, Thermodynamics of the quantum mpemba effect, *Physical Review Letters* **133**, 140404 (2024).
- [22] A. Nava and R. Egger, Mpemba effects in open nonequilibrium quantum systems, *Physical Review Letters* **133**, 136302 (2024).
- [23] A. K. Chatterjee, S. Takada, and H. Hayakawa, Quantum mpemba effect in a quantum dot with reservoirs, *Physical Review Letters* **131**, 080402 (2023).
- [24] D. J. Strachan, A. Purkayastha, and S. R. Clark, Non-markovian quantum mpemba effect, *Physical Review Letters* **134**, 220403 (2025).
- [25] A. K. Chatterjee, S. Takada, and H. Hayakawa, Multiple quantum mpemba effect: Exceptional points and oscillations, *Physical Review A* **110**, 022213 (2024).
- [26] F. Ares, S. Murciano, and P. Calabrese, Entanglement asymmetry as a probe of symmetry breaking, *Nature Communications* **14**, 2036 (2023).
- [27] X. Turkeshi, P. Calabrese, and A. De Luca, Quantum mpemba effect in random circuits, *Physical Review Letters* **135**, 040403 (2025).
- [28] S. Yamashika, F. Ares, and P. Calabrese, Entanglement asymmetry and quantum mpemba effect in two-dimensional free-fermion systems, *Physical Review B* **110**, 085126 (2024).
- [29] S. Yamashika and F. Ares, Quantum mpemba effect in long-range spin systems, *Physical Review Letters* **136**, 090402 (2026).
- [30] S. Murciano, F. Ares, I. Klich, and P. Calabrese, Entanglement asymmetry and quantum mpemba effect in the xy spin chain, *Journal of Statistical Mechanics: Theory and Experiment* **2024**, 013103 (2024).
- [31] S. Liu, H.-K. Zhang, S. Yin, and S.-X. Zhang, Symmetry restoration and quantum mpemba effect in symmetric random circuits, *Physical Review Letters* **133**, 140405 (2024).
- [32] C. Rylands, K. Klobas, F. Ares, P. Calabrese, S. Murciano, and B. Bertini, Microscopic origin of the quantum mpemba effect in integrable systems, *Physical Review Letters* **133**, 010401 (2024).
- [33] M. Rigol, V. Dunjko, and M. Olshanii, Thermalization and its mechanism for generic isolated quantum systems, *Nature* **452**, 854 (2008).
- [34] J. Eisert, M. Friesdorf, and C. Gogolin, Quantum many-body systems out of equilibrium, *Nature Physics* **11**, 124 (2015).
- [35] V. Gorini, A. Kossakowski, and E. C. G. Sudarshan, Completely positive dynamical semigroups of n-level systems, *Journal of Mathematical Physics* **17**, 821 (1976).
- [36] G. Lindblad, On the generators of quantum dynamical semigroups, *Communications in Mathematical Physics* **48**, 119 (1976).
- [37] D. Ruelle, Resonances of chaotic dynamical systems, *Physical Review Letters* **56**, 405 (1986).
- [38] M. Pollicott, On the rate of mixing of axiom a flows, *Inventiones Mathematicae* **81**, 413 (1985).
- [39] T. Prosen, Ruelle resonances in quantum many-body dynamics, *Journal of Physics A: Mathematical and General* **35**, L737 (2002).
- [40] M. Žnidarič, Momentum-dependent quantum ruelle-pollicott resonances in translationally invariant many-body systems, *Physical Review E* **110**, 054204 (2024).
- [41] T. Mori, Liouvillian-gap analysis of open quantum many-body systems in the weak dissipation limit, *Physical Review B* **109**, 064311 (2024).
- [42] X. Mi, M. Ippoliti, C. Quintana, A. Greene, Z. Chen, J. Gross, F. Arute, K. Arya, J. Atalaya, R. Babush, J. C. Bardin, J. Basso, A. Bengtsson, A. Bilmes, A. Bourassa, L. Brill, M. Broughton, B. B. Buckley, D. A. Buell, B. Burkett, N. Bushnell, B. Chiaro, R. Collins, W. Courtney, D. Debroy, S. Demura, A. R. Derk, A. Dunsworth, D. Eppens, C. Erickson, E. Farhi, A. G. Fowler, B. Foxen, C. Gidney, M. Giustina, M. P. Harrigan, S. D. Harrington, J. Hilton, A. Ho, S. Hong, T. Huang, A. Huff, W. J. Huggins, L. B. Ioffe, S. V. Isakov, J. Iveland, E. Jeffrey, Z. Jiang, C. Jones, D. Kafri, T. Khattar, S. Kim, A. Kitaev, P. V. Klimov, A. N. Korotkov, F. Kostritsa, D. Landhuis, P. Laptev, J. Lee, K. Lee, A. Locharla, E. Lucero, O. Martin, J. R. McClean, T. McCourt, M. McEwen, K. C. Miao, M. Mohseni, S. Montazeri, W. Mruczkiewicz, O. Naaman, M. Neeley, C. Neill, M. Newman, M. Y. Niu, T. E. O'Brien, A. Opremcak, E. Ostby, B. Pato, A. Petukhov, N. C. Rubin, D. Sank, K. J. Satzinger, V. Shvarts, Y. Su, D. Strain, M. Szalay, M. D. Trevithick, B. Villalonga, T. White, Z. J. Yao, P. Yeh, J. Yoo, A. Zalcman, H. Neven, S. Boixo, V. Smelyanskiy, A. Megrant, J. Kelly, Y. Chen, S. L. Sondhi, R. Moessner, K. Kechedzhi, V. Khemani, and P. Roushan, Time-crystalline eigenstate order on a quantum processor, *Nature* **601**, 531 (2021).
- [43] J. Zhang, P. W. Hess, A. Kyprianidis, P. Becker, A. Lee, J. Smith, G. Pagano, I.-D. Potirniche, A. C. Potter, A. Vishwanath, N. Y. Yao, and C. Monroe, Observation of a discrete time crystal, *Nature* **543**, 217 (2017).
- [44] K. Seki, Y. Kikuchi, T. Hayata, and S. Yunoki, Simulating floquet scrambling circuits on trapped-ion quantum computers, *Physical Review Research* **7**, 023032 (2025).
- [45] U. Duh and M. Žnidarič, [arXiv:2506.24097](https://arxiv.org/abs/2506.24097).
- [46] L. D'Alessio and M. Rigol, Long-time behavior of isolated periodically driven interacting lattice systems, *Physical Review X* **4**, 041048 (2014).
- [47] C. Fleckenstein and M. Bukov, Thermalization and

prethermalization in periodically kicked quantum spin chains, [Physical Review B **103**, 144307 \(2021\)](#).

[48] C. M. Bender and S. A. Orszag, *Advanced Mathematical Methods for Scientists and Engineers I: Asymptotic*

Methods and Perturbation Theory, 1st ed. (Springer, New York, 1999).

[49] G. H. Hardy and E. M. Wright, *An introduction to the theory of numbers* (Oxford university press, 1979).

Supplemental Information

I. ASYMPTOTIC ANALYSIS OF THE REDUCED DENSITY MATRIX

We analyse the large-time behaviour of the reduced density matrix in the form

$$\rho_s(t) - \frac{I}{2^\ell} = \sum_\alpha \int_{-\pi}^{\pi} \frac{dk}{2\pi} \lambda_{\alpha,k}^t \text{Tr}[\rho(0)V_{\alpha,k}^R] \varrho_{\alpha,k}. \quad (\text{SM-1})$$

As argued in the main text, when $\rho(0)$ has a finite spatial periodicity, $\text{Tr}[\rho(0)V_{\alpha,k}^R]$ reduces to the sum of delta functions, and equation (SM-1) becomes a discrete sum, leading to purely exponential relaxation. Here we focus on the opposite case in which $\rho(0)$ has no finite spatial periodicity, i.e., the translational symmetry is completely broken.

It is convenient to rewrite $\lambda_{\alpha,k}$ as

$$\lambda_{\alpha,k} = e^{-\nu_{\alpha,k}}, \quad (\text{SM-2})$$

Then, equation (SM-1) becomes

$$\rho_s(t) - \frac{I}{2^\ell} = \sum_\alpha \int_{-\pi}^{\pi} \frac{dk}{2\pi} e^{-t\nu_{\alpha,k}} \text{Tr}[\rho(0)V_{\alpha,k}^R] \varrho_{\alpha,k}. \quad (\text{SM-3})$$

At large t , the integral is dominated by the neighbourhood of the points at which $\Re(\nu_{\alpha,k})$ attains local minima and equivalently $|\lambda_{\alpha,k}|$ attains local maxima. If we denote as Σ_α the set of such points, in the vicinity of $k = q \in \Sigma_\alpha$, we obtain

$$\nu_{\alpha,k} \simeq \nu_{\alpha,q} + \nu'_{\alpha,q}(k - q) + \frac{\nu''_{\alpha,q}}{2}(k - q)^2, \quad (\text{SM-4})$$

with $\Re(\nu'_{\alpha,q}) = 0$ and $\Re(\nu''_{\alpha,q}) > 0$. Let $\gamma_q \in \mathbb{Z}_{\geq 0}$ be the smallest integer such that

$$\text{Tr}[\rho(0)V_{\alpha,k}^R] = \eta_\alpha |k - q|^{\gamma_q} + O(|k - k_q|^{\gamma_q+1}), \quad \eta_\alpha \neq 0. \quad (\text{SM-5})$$

Substituting equations (SM-4) and (SM-5) into equation (SM-1), we obtain

$$\rho_s(t) - \frac{I}{2^\ell} \simeq \sum_\alpha \sum_{q \in \Sigma_\alpha} \lambda_{\alpha,q}^t \eta_{\alpha,q} \varrho_{\alpha,q} \int_{\mathbb{R}} \frac{dk}{2\pi} |k|^{\gamma_q} e^{-t\nu'_{\alpha,q}k - \frac{t}{2}\nu''_{\alpha,q}k^2}. \quad (\text{SM-6})$$

Here, we extended the integral domain to $k \in \mathbb{R}$ as the integrand is exponentially small away from $k = q \in \Sigma_\alpha$. The integral over k in the above equation can be easily taken by the standard mean of the Gaussian integral, which results in

$$\rho_s(t) - \frac{I}{2^\ell} \simeq \sum_\alpha \sum_{k \in \Sigma_\alpha} \lambda_{\alpha,k}^t \eta_{\alpha,k} \varrho_{\alpha,k} \begin{cases} -\frac{\Gamma(1 + \gamma_k) \sin(\frac{\gamma_k \pi}{2})}{\pi |\nu'_{\alpha,k}|^{1+\gamma_k} t^{1+\gamma_k}} & \nu'_{\alpha,k} \neq 0 \wedge \gamma_k = \text{odd} \\ \frac{\left(-\frac{\nu'_{\alpha,k}}{\nu''_{\alpha,k}}\right)^{\gamma_k} \exp\left(-\frac{t|\nu'_{\alpha,k}|^2}{2\nu_{\alpha,k}}\right)}{\sqrt{2\pi t \nu''_{\alpha,q}}} & \nu'_{\alpha,k} \neq 0 \wedge \gamma_k = \text{even} , \\ \frac{1}{2\pi} \Gamma\left(\frac{1 + \gamma_k}{2}\right) \left(\frac{2}{\nu''_{\alpha,k} t}\right)^{\frac{1+\gamma_k}{2}} & \nu'_{\alpha,k} = 0 \end{cases} \quad (\text{SM-7})$$

where $\Gamma(x)$ is the Gamma function. When $\text{Tr}[\rho(0)V_{\alpha,q}^R] \neq 0$ one has $\gamma_q = 0$ and the above equation reduces to equation (9) in the main text.

II. ACCELERATED RELAXATION IN THE KICKED ISING CHAIN

In Sec. I, we found that the relaxation law depends on γ when the overlap factor vanishes as $\text{Tr}[\rho(0)V_{\alpha,k}^R] \simeq \eta_k |k - q|^\gamma$ in the vicinity of $k = q \in \Sigma_\alpha$. Here, we provide an explicit example in which this effect appears in the dynamics of the kicked Ising chain.

For the kicked Ising chain, since $|\lambda_{\alpha,k_\alpha}| < 1$ for all k and $|\lambda_{1,k}|$ attains its global maximum at $k = 0$ with $\lambda_{1,k} \in \mathbb{R}$ in the vicinity of $k = 0$, equation (SM-6) reduces to

$$\rho_s - \frac{I}{2^\ell} \simeq \frac{\eta_1 \lambda_{1,0}^t \Gamma(\frac{1+\gamma}{2}) \varrho_{1,0}}{2\pi [t\nu''_{1,0}/2]^{\frac{1+\gamma}{2}}}. \quad (\text{SM-8})$$

Therefore, the accelerated relaxation with the enhanced power $\sim t^{-(1+\gamma)/2}$ with $\gamma > 0$ is realised when the initial state satisfies

$$\text{Tr}[\rho(0)V_{1,0}^R] = \sum_{P \in \mathcal{P}_\infty} v_{1,P_0}^R \text{Tr}[\rho(0)P_0] = 0, \quad (\text{SM-9})$$

where $P_0 = \sum_{j \in \mathbb{Z}} \mathcal{T}^j P$. Equation (SM-9) follows if $\text{Tr}[\rho(0)P_0] = 0$ for all P . Such an initial state can be constructed from a de Bruijn sequence [2]: Let $\{b_n\}_{n=0}^{L-1}$ be a binary de Bruijn sequence of order r_d , i.e., a cyclic binary string of length $L = 2^{r_d}$ in which every binary word of length r_d appears exactly once as a contiguous substring. For example, for $r_d = 3$,

$$\{b_n\}_{n=0}^7 = 00010111, \quad (\text{SM-10})$$

which contains each of the length-3 substrings

$$000, 001, 010, 101, 111, 110, 100, \quad (\text{SM-11})$$

exactly once when read cyclically.

Using this sequence, we take as the initial state the computational-basis product state

$$\rho(0) = \bigotimes_{n=0}^{L-1} |b_n\rangle \langle b_n|. \quad (\text{SM-12})$$

By construction, for any Pauli string supported on at most r_d consecutive sites, the translation average $P_0 = \sum_{j=0}^{L-1} \mathcal{T}^j P$ has vanishing expectation value in $\rho(0)$. Indeed, if P contains X or Y on any site then each term $\text{Tr}[\rho(0)\mathcal{T}^j P]$ vanishes individually because $\rho(0)$ is diagonal in the computational basis. If P consists only of I and Z , then $\text{Tr}[\rho(0)\mathcal{T}^j P] = \pm 1$ depends only on the length- r_d substring of $\{b_n\}$ starting at j -th qubit. Since all such substrings appear exactly once in the de Bruijn sequence, the sum over j cancels exactly, yielding $\text{Tr}[\rho(0)P_0] = 0$. Although $\text{Tr}[\rho(0)P_0] = 0$ does not hold for the Pauli strings whose lengths are larger than $r_d = \log_2 L$, this property of de Bruijn sequence with finite r_d is expected to suppress $\text{Tr}[\rho(0)V_{1,0}^R]$ and thereby realise $\gamma \geq 1$ approximately. Figure SM-1 plots the resulting time evolution of the Bures distance between the equilibrium state and the reduced density matrix for the kicked Ising dynamics starting from the initial state (SM-12), exhibiting a decay consistent with $D(t) = O(|\lambda_{1,0}|^t t^{-1})$. This corresponds to $\gamma = 1$, i.e., a faster approach to equilibrium than in the $\gamma = 0$ cases discussed in the main text.

1. C. M. Bender and S. A. Orszag, *Advanced Mathematical Methods for Scientists and Engineers I: Asymptotic Methods and Perturbation Theory*, 1st ed. (Springer, New York, 1999).
2. N. G. de Bruijn and P. Erdős, *On a combinatorial problem*, Proceedings of the Section of Sciences of the Koninklijke Nederlandse Akademie van Wetenschappen te Amsterdam, **51**(10), 1277-1279 (1948).

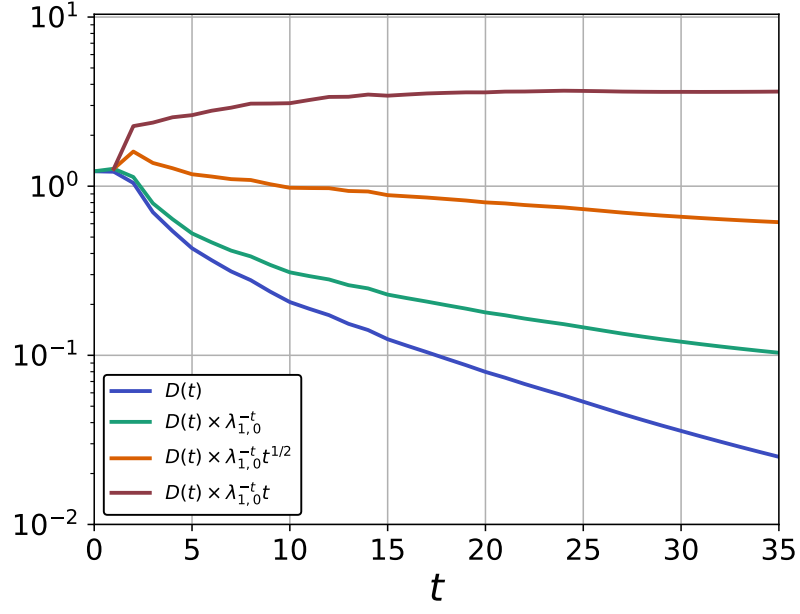


FIG. SM-1. The time evolution of the Bures distance $D(t)$ for the dynamics starting from the initial state (SM-12) generated from the de Bruijn sequence with $r_d = 5$, which corresponds to $L = 2^{r_d} = 32$ qubits. We find that the decay of $D(t)$ is consistent with Eq. (SM-8) with $\gamma = 1$, which corresponds to the faster decay than that discussed in the main text.